

Maintenance of ATP favours apoptosis over necrosis triggered by benzamide riboside

M Grusch¹, D Polgar¹, S Gfatter², K Leuhuber³,
S Huettenbrenner¹, C Leisser¹, G Fuhrmann¹, F Kassie²,
H Steinkellner², K Smid⁴, GJ Peters⁴, HN Jayaram⁵,
W Klepal³, T Szekeres⁶, S Knasmüller² and G Krupitza^{*1}

¹ Institute of Clinical Pathology, University of Vienna, Austria

² Institute for Cancer Research, University of Vienna, Austria

³ Institute of Zoology, University of Vienna, Austria

⁴ Department of Medical Oncology, University Hospital VU Amsterdam, The Netherlands

⁵ Department of Biochemistry and Molecular Biology and Laboratory for Experimental Oncology, Indiana University School of Medicine, Indianapolis, USA

⁶ Clinical Institute of Medical and Chemical Laboratory Diagnosis, University of Vienna, Austria

* Corresponding author: G Krupitza, Institute of Clinical Pathology, Waehringer Guertel 18-20, A-1090 Vienna, Austria. Tel: 0043 1 40400 3487; Fax: 0043 1 405 34 02; E-mail: g.krupitza@akh.wien.ac.at

Received 6.6.01; revised 31.7.01; accepted 1.8.01

Edited by RA Knight

Abstract

A new synthetic drug, benzamide riboside (BR) exhibited strong oncolytic activity against leukemic cells in the 5–10 μM range. Higher BR-concentrations (20 μM) predominantly induced necrosis which correlated with DNA strand breaks and subsequent depletion of ATP- and dATP levels. Replenishment of the ATP pool by addition of adenosine prevented necrosis and favoured apoptosis. This effect was not a peculiarity of BR-treatment, but was reproduced with high concentrations of all-trans-retinoic acid (120 μM) and cyanide (20 mM). Glucose was also capable to suppress necrosis and to favour apoptosis of HL-60 cells, which had been treated with necrotic doses of BR and cyanide. Apoptosis eliminates unwanted cells without affecting the microenvironment, whereas necrosis causes severe inflammation of surrounding tissues due to spillage of cell fluids into the peri-cellular space. Thus, the monitoring and maintenance of cellular energy pools during therapeutic drug treatment may help to minimize nonspecific side effects and to improve attempted drug effects.

Cell Death and Differentiation (2002) 9, 169–178. DOI: 10.1038/sj/cdd/4400937

Keywords: benzamide riboside; apoptosis; necrosis; ATP

Abbreviations: ATP, adenosine triphosphate; ATRA, all-trans retinoic acid; BR, 3-(1- β -D-ribofuranosyl)benzamide or benzamide riboside; dATP, 2'-deoxyadenosine 5'-triphosphate; dGTP, 2'-deoxyguanosine 5'-triphosphate; DTT, DL-dithiothreitol; EDTA,

ethylenediaminetetraacetic acid; FCS, foetal calf serum; GTP, guanosine 5'-triphosphate; IMP, inosine 5'-monophosphate; IMPDH, inosine 5'-monophosphate dehydrogenase; HO, Hoechst 33258; KCN, potassium cyanide; NAD, nicotinamide adenine dinucleotide; PARP, poly(ADP-ribose)polymerase; PBS, phosphate-buffered saline; PI, propidium iodide; RR, ribonucleotide reductase; SCGE, single cell gel electrophoresis or comet assay; SDS, sodium dodecyl sulfate; TCA, trichloro acetic acid; TEM, transmission electron microscopy; TR, 2- β -D-ribofuranosylthiazole-4-carboxamide or tiazofurin; XMP, xanthosine 5'-monophosphate

Introduction

Benzamide riboside (BR) is a C-nucleoside¹ that has recently been characterised as an inosine 5'-monophosphate dehydrogenase (IMPDH)-inhibitor.^{2,3} This enzyme catalyses the conversion of IMP to xanthosine 5'-monophosphate (XMP) and is the rate limiting enzyme in *de novo* guanylate biosynthesis.⁴ The activity of this enzyme is significantly increased in tumour cells and therefore considered to be a potential target for cancer chemotherapy.⁵ Tiazofurin (TR), which is metabolized in a similar manner to that of BR, was found to inhibit the growth of human myelogenous leukaemia K562⁶ and human promyelocytic leukaemia HL-60 cells.⁷ TR is an inhibitor of IMPDH⁸ and Phase I/II clinical trials conducted with this compound in acute myelogenous leukaemia patients, indicated a significant reduction in leukaemic cell burden.^{9–11} BR, exhibited stronger antiproliferative activity in the K562 cells than TR¹² and was shown to induce apoptosis in HL-60¹³ and N.1 ovarian carcinoma cells.^{13,14} Higher BR-concentrations however, provoked necrosis, which is a common phenomenon of pro-apoptotic drugs^{15–17} and limits chemotherapy because of non-specific drug toxicity. Overdosing results in necrosis and spilling of intracellular fluids into the peri-cellular space, leading to inflammatory responses with wide ranging destructions of surrounding tissues. Therefore it is of prime interest to develop strategies to suppress necrosis and favour apoptosis. Interestingly, both cell death modes, apoptosis and necrosis, were discussed to partly share similar early pathways.^{17–19}

It was postulated that BR exerts its anti-tumour effects due to IMPDH inhibition.^{2,12} Therefore dGTP and other dNTP levels were analyzed and correlated with cell death modes. The necrotic trigger of high BR-concentrations was identified as DNA-clastogenic activity, which subsequently led to ATP depletion. It is likely that ATP levels are the key factor deciding the death modes, because apoptosis is energy- (ATP-) dependent, whereas necrosis is not. Here we describe a new strategy to reduce non-specific toxicity by drug-overload, by artificially keeping ATP levels high and to specifically promote apoptosis and prevent necrosis.

Results

The BR concentrations determines the type of cell death

Treatment of HL-60 cells with increasing doses of BR induced cell death which was analyzed by Trypan blue staining (data not shown).²⁰ To further discriminate the type of cell death, the integrity of poly(ADP-ribose) polymerase [PARP] and gelsolin was examined by Western blotting (Figure 1). PARP and Gelsolin become signature-specifically fragmented by Caspase 3 upon induction of apoptosis. Addition of 0.5 μM , 1 μM , or 2 μM BR neither induced cell death nor gelsolin cleavage, whereas concentrations of 5 μM or 10 μM BR caused apoptosis which was evidenced by degradation of gelsolin into a 41 kD fragment²¹ and of PARP into a 89 kD fragment (Figure 1a,b). Further increase of the BR-concentrations to 20 μM led to an increase of the fraction of necrotic cells and reduced the fraction of apoptotic cells, which was also reflected by the lack of PARP and gelsolin fragmentation.

HL-60 cells treated with 5 μM BR or 20 μM BR for 24 h exhibited typical apoptotic or necrotic morphologies, respectively, which was examined by electron microscopy (Figure 2). The untreated control cell (Figure 2a) was characterised by an intact cell membrane and nuclear envelope and a normal chromatin distribution. HL-60 cells treated with 5 μM BR (Figure 2b) still maintained intact membranes but electron dense chromatin margined at the nuclear envelope as a hallmark of apoptosis. The vacuoles

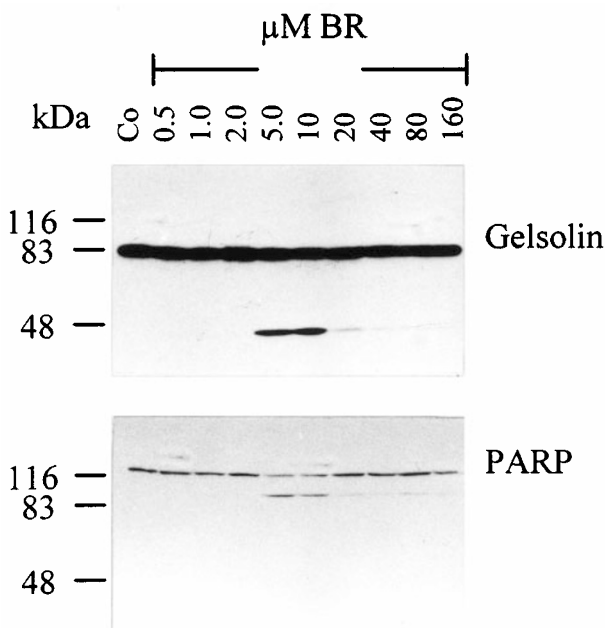


Figure 1 Cleavage of the caspase substrate poly(ADP-ribose) polymerase (PARP) (A) and gelsolin (B) following treatment of HL-60 cells with increasing doses of BR. Controls were treated with saline for 24 h and Western blots were performed as described in Materials and Methods. The 89 kD cleavage product of PARP and the 41 kD cleavage product of gelsolin could be detected upon treatment with 5 μM and 10 μM BR and diminished in response to higher doses of BR

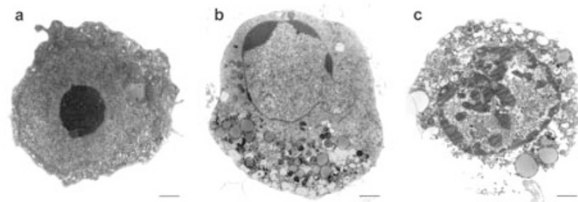


Figure 2 Electron microscopical images of apoptotic and necrotic HL-60 cells. HL-60 cells were treated with saline (A), 5 μM BR (B), and 20 μM BR (C) for 24 h, and prepared for electron microscopical analysis as described in Materials and Methods. Panel A shows an intact cell morphology, panel B an apoptotic cell with typical DNA condensation and margination at the nuclear envelope and panel C a necrotic cell exhibiting cloudy chromatin and destructed organelles and membranes. The bars at the lower right corners indicate 1.1 μm

in the cytoplasm seemed to enlarge during BR treatment. HL-60 cells treated with 20 μM BR (Figure 2c) exhibited typical necrotic morphology such as disrupted membranes and cloudy chromatin.

Measurement of dNTP- and ATP-levels

The dNTP levels were determined after 16 h treatment. At this time point cells were still viable and membranes intact, preventing nonspecific loss of dNTPs.²²

Table 1 shows that 5 μM BR and 20 μM BR repressed dGTP levels to similar extent (approximately 53% of control). The cellular dGTP concentrations did not correlate with induction of apoptosis or necrosis by 5 μM BR and 20 μM BR respectively, after 16, 24 or 48 h of treatment (compare with Figure 3a). Whereas dCTP (89% of control) – and dATP (81% of control) – levels were in the range of control when cells were treated with 5 μM BR, exposure to 20 μM BR caused a drop in dCTP and dATP levels to 37 and 33%, respectively.

It was assumed that ATP level is a determinant of cell death modes.^{15,23–25} Hence, we determined the ATP levels in HL-60 cells (Figure 3b) after treatment with 5 μM BR (which causes apoptosis) and after exposure to 20 μM BR (which mainly causes necrosis) (Figure 3a). In case ATP determines the type of cell death, then it has to be a regulatory parameter before cell death (apoptosis and/or necrosis) occurs. Therefore, the intracellular ATP pools were examined after 16 h of treatment (Figure 3b), when the cell membranes were still intact and no non-specific loss of nucleotides took place. Treatment with a membrane permeable ATP-precursor, adenosine, was expected to replenish the intracellular pools of ATP and to inhibit necrosis. In fact, addition of 800 μM adenosine rescued the ATP levels in 20 μM BR treated cells to 31% of the control value, whereas a dramatic ATP drop to 2.7% of control was seen, when cells were exposed to 20 μM BR only (Figure 3b). In the adenosine-treated cells necrosis was indeed inhibited (Figure 3a). Figure 3c shows HOPI double-stained viable cells, early and late apoptotic cells and necrotic HL-60 cells, which were exposed to 5 μM and 20 μM BR, with or without adenosine (panel A). For reasons of comparison, panel B depicts necrotic HL-60 cells which

Table 1 dNTP levels in response to treatment of HL-60 cells with benzamide riboside

HL-60	dATP	dTTP	dCTP	dGTP	Apoptosis
Control (100%)	10.6 pm (+1.0, -0.7)	18.2 pm (+7.9, -5.1)	9.1 pm (+1.0, -1.9)	9.1 pm (+1.8, -1.2)	1%
5 μ M BR	81.3%	252.1%	89.5%	52.6%	4%
20 μ M BR	32.6%	148.4%	36.7%	53.8%	18%
Co+A	69.9%	113.6%	64.3%	39.8%	9%
5 μ M BR+A	76.1%	327.8%	117.1%	29.5%	11%
20 μ M BR+A	65.1%	177.7%	58.4%	29.6%	7%

HL-60 cells were treated with increasing doses of benzamide riboside (BR) for 16 h. Then the cells were lysed, and dNTPs isolated and analyzed as described in Materials and Methods. Values are given in picomol (pm) of each dNTP per 1×10^6 cells for controls, and as per cent of control for treated samples

underwent heat shock treatment (55°C) for increasing times and panel C demonstrates the lack of PARP cleavage after heat shock (Figure 3c). Re-directing necrosis to apoptosis was also reflected by Caspase 3 cleavage to its active form in presence of 800 μ M adenosine in HL-60 cells which were treated with 20 μ M BR (Figure 3d). Whereas Caspase 3 activation culminated (p20 kD fragment) after exposure to 5 μ M and 10 μ M BR after 24 h, activation was inhibited after exposure to 20 μ M or 40 μ M BR. In contrast, more of the activated Caspase 3-fragment was detected after 20 μ M and 40 μ M BR-treatment in presence of 800 μ M adenosine. Lower adenosine levels had no effect probably due to limits in cellular uptake or due to specific degradation by adenosine deaminase.

ATP-, dATP-, and dCTP-levels correlate with apoptosis

To elucidate, whether a direct correlation exists between nucleotide pools and death modes, ATP, dATP and dCTP levels were plotted in combination with the corresponding apoptosis- and necrosis-rates. For improved comprehension we summarised in Table 2 the ATP-, dATP-, dCTP-levels and death data and graphically compared the inter-relationships of total cell deaths, the apoptotic- and the necrotic subtypes with nucleotide levels from differently treated cells. It can be seen in Figure 4a, b and c that ATP-, dATP-, and dCTP levels directly correlate with apoptosis rates and inversely with the necrosis rates, when cell death was induced by BR (not however in non-induced cells such as control or adenosine control; not shown in Figure 4a–c). There was no correlation of ATP or dATP levels with total cell deaths (apoptosis+ necrosis; not shown).

Apoptosis is an energy dependent process, because to maintain membrane integrity ATP is required. Since adenosine restored the ATP pool and prevented necrosis also glucose was anticipated to prevent necrosis^{18,25–27} and to determine death modes. In fact 100 mM glucose nearly completely inhibited necrosis of HL-60 cells induced by treatment with 20 μ M BR and instead favoured apoptosis, which was determined by HOPI double-staining.^{13,22,28} In these experiments spontaneous cell death of controls exhibited an apoptosis:necrosis-ratio A:N=3.6:1. 20 μ M BR resulted in a ratio A:N=1:3.4, which was converted by the addition of glucose to a ratio A:N=7.8:1.

Adenosine prevents ATRA- and KCN-triggered necrosis in favour of apoptosis

To examine, whether prevention of necrosis by energy donors was a peculiarity of BR-induced cell death, or it represents a more general mechanism, HL-60 cells were treated with all-trans retinoic acid (ATRA) and potassium cyanide (KCN). ATRA is used clinically to treat acute promyeloid leukaemia.²⁹ KCN blocks the respiratory chain and prevents ATP generation.^{30–32} Exposure of the cells to 120 μ M ATRA for 48 h resulted in 30% apoptotic and 45% necrotic cells (apoptosis:necrosis ratio A:N=1:1.5) (Figure 5). Addition of 100 mM glucose repressed both apoptosis and necrosis (A:N=1:1.2). Also 800 μ M adenosine repressed both types of cell death, but in this case the apoptosis rate was increased (A:N=1.8:1). The effect of glucose and adenosine on KCN-induced cell death was even more dramatic: 20 mM KCN alone caused 32% apoptosis and 41% necrosis after 48 h of treatment (A:N=1:1.3) in HL-60 cells. Addition of 100 μ M glucose did not suppress KCN-induced cell death, as in the case with ATRA, and inverted the death ratio in favour of apoptosis (A:N=1.7:1). 800 μ M adenosine substantially suppressed necrosis and increased the apoptosis rate to 43% (A:N=9.1:1) (Figure 5).

Necrotic BR-concentrations induce DNA double-strand breaks

DNA integrity was measured in individual cells with the single cell gel electrophoresis (comet) assay. The analyses were performed at time points (8 and 16 h of treatment with BR), when the cell membranes were still intact and before apoptotic or necrotic markers were observed, but when ATP- and dNTP-pools were already affected. The results of comet assays performed at neutral pH (7.5) showed that 20 μ M BR, but not 5 μ M BR, induced DNA double-strand breaks within 8 h of treatment. These breaks were efficiently repaired after 16 h (Figure 6a). Additional comet-analyses at alkaline pH (13.0) demonstrated also that DNA single-strand breaks occurred after incubation with 20 μ M BR, but not with 5 μ M BR treatment. These lesions were substantially, but not completely repaired after 16 h (Figure 6b). The ATP level after 16 h of treatment with 20 μ M BR (3% control) seemed to be insufficient for the repair of the remaining DNA single-strand breaks, and this might have resulted in necrosis. These results also suggest that 5 μ M BR-induced apoptosis

is not causally related to DNA double- or single-strand breaks.

Viable and pre-apoptotic cells contain (relatively) high ATP levels in contrast to pre-necrotic cells. Therefore, we compared cells with high *versus* low ATP content with the extent of DNA damage after 16 h of treatment. Comet analysis at alkaline pH (13.0) revealed that the combined percentage of surviving+apoptotic cells (98% of the cells after each exposure to either 5 μ M BR or 5 μ M BR+adenosine) corresponded to a 25 μ m DNA tail length (96 and 95%, respectively, see Table 2). Whereas the percentage of necrotic cells (51% after treatment with 20 μ M BR) correlated with cells with a >25 μ m DNA tail length (50%) (Table 2, Figure 6b). The inclusion of adenosine promoted DNA repair of a subset of 20 μ M BR-treated cells after 16 h. However, in 26% of the 20 μ M BR-damaged cells DNA-single-strand breaks also accumulated after 16 h when co-treated with adenosine, because DNA tail lengths increased (100–140 μ m) (Figure 6b). The combined percentages (68%; viable+apoptotic) of 20 μ M BR+adenosine treated cells did not correlate with the percentage of cells with a DNA tail length <25 μ m (45%) (Table 2, Figure 6b). This demonstrates that adenosine allowed ~23% of the cells, which still had substantially damaged DNA and that were otherwise prone for necrosis (DNA tail length >25 μ m, <87 μ m), to undergo apoptosis.

3-amino benzamide (3-AB) represses necrosis

Since 20 μ M BR dramatically depleted the ATP pool to 3% of control we speculated that this might have been due to DNA strand break-dependent activation of poly(ADP-ribose)polymerase (PARP). PARP consumes NAD and in consequence also affects the ATP pool.^{33,34} Moreover, PARP activity was shown to provoke necrosis^{23,35,36} and in PARP(–/–) mice upon cerebral ischemia reperfusion necrotic cell death did not occur.³⁷ 3-AB is a potent inhibitor of PARP, and in fact, we found that 20 μ M BR-induced necrosis was inhibited in presence of 2 mM 3-AB (Figure 7). This supports the

assumption that PARP-activation might provoke BR-induced necrosis due to energy depletion, which is prevented by PARP-inhibition.

Discussion

It is a well known phenomenon that cytotoxic drugs, which can induce apoptosis, promote necrosis when administered at higher concentrations.^{15–17,38} Several reports suggest that apoptosis and necrosis share, in part, similar (early) pathways of induction.^{17–19,39} Also p53 might determine whether a death pathway can be completed by apoptosis or whether mutated p53 allows only for a necrotic fate at equitoxic concentrations.

It was suggested that the intracellular ATP level determines whether a cell dies in an apoptotic or necrotic mode.^{15,23–25} Therefore, we investigated ATP levels in benzamide riboside (BR)-treated HL-60 cells, which apoptosed after 5 μ M treatments, whereas they underwent necrosis at 20 μ M BR treatment. BR is a new synthetic C-nucleoside,¹ which inhibits IMPDH, the rate limiting enzyme of *de novo* guanylate biosynthesis. IMPDH is frequently over-expressed in cancer cells and therefore, considered a target for anti-tumour therapy. It was previously demonstrated that BR exhibits strong anti neoplastic activity in a panel of human tumour cell lines³ and was most effective in leukaemia cells by inducing apoptosis.^{13,14,40} The oncolytic activity of BR³ was assumed to be due to its IMPDH-inhibitory and, therefore, dGTP-limiting action.^{2,12} This hypothesis was strongly encouraged by the observation, that guanosine, a precursor of dGTP, prevented the oncolytic activity of BR.^{12,41}

Our findings show, that 5 μ M BR induced apoptosis, whereas 20 μ M BR provoked necrosis, although both concentrations of BR inhibited dGTP synthesis to a similar degree. dGTP levels were comparably affected by adenosine, which only marginally interfered with cell survival (see Table 2). Therefore, it seems unlikely that dGTP depletion alone accounted for the cell death mechanism elicited by BR. BR-mediated limitation of dGTP

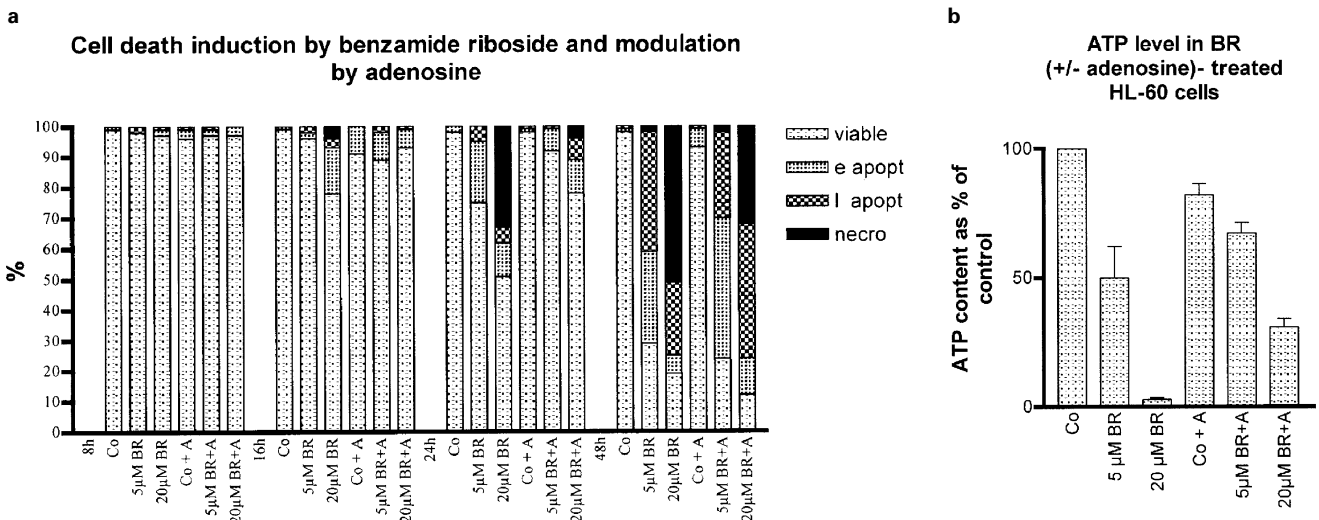


Table 2 Comparison of dNTP levels with DNA tail lengths and cell status

	% ATP	% dATP	% dCTP	DNA tail length	% viable	% apopt	% viable +apopt	% necro	% total death
Control	100	100	100	98% <=25 μ m	98	2	100	0	2
Ade	85	70	64	98% <=25 μ m	93	7	100	0	7
5 μ M BR	50	81	89	96% <=25 μ m	29	69	98	2	71
20 μ M BR	3	33	37	50% <=25 μ m 50% >=25 μ m	19	30	49	51	81
5 μ M BR+Ade	68	76	117	95% <=25 μ m	24	74	98	2	76
20 μ M BR+Ade	31	56	58	45% <=25 μ m 55% >=25 μ m	12	56	68	32	88

The percentages of ATP, dATP and dCTP levels and the DNA tail length of HL-60 cells after 16 h of BR±adenosine treatment, and the percentages of viable, apoptotic and necrotic cells following treatment for 48 h with BR±adenosine, were measured. Viable cells displayed nuclei homogeneously stained with Hoechst and excluded PI. Apoptotic cells showed chromatin condensation and nuclear fragmentation. At least 200 cells were counted from each sample

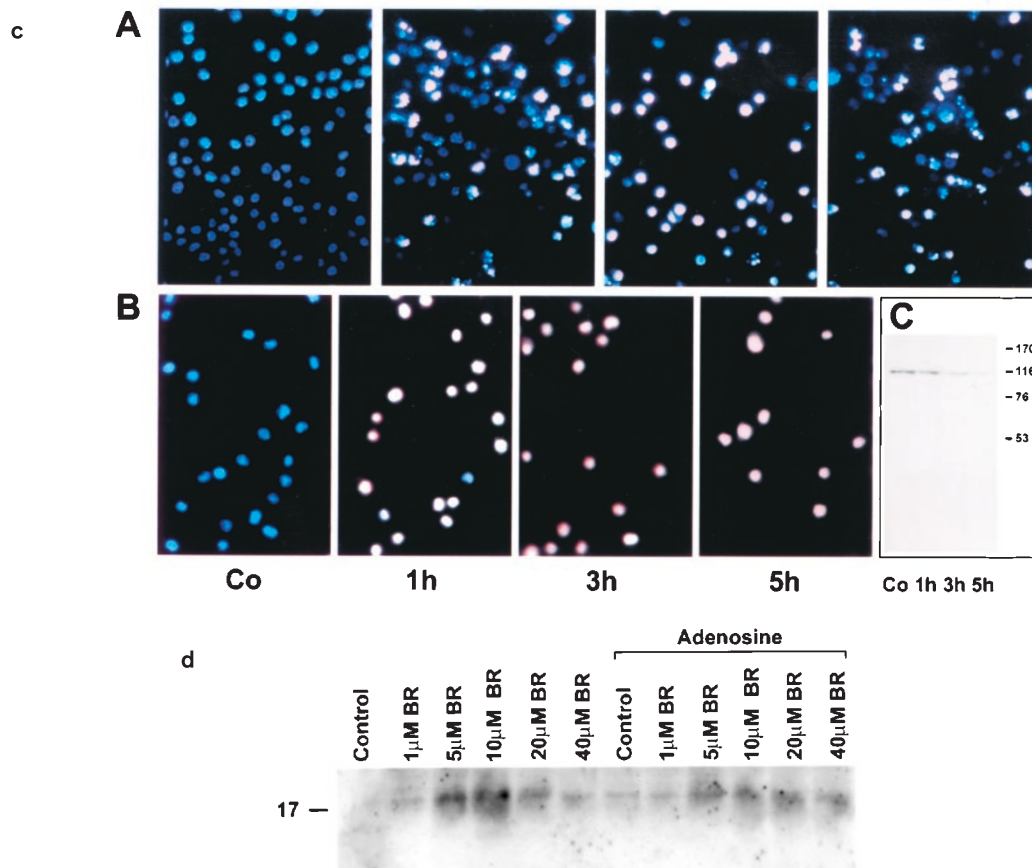


Figure 3 Induction of cell death modes by BR. (a) Cells were treated with saline (Co), 800 μ M adenosine (Co+A), 5 μ M BR (\pm adenosine), 20 μ M BR (\pm adenosine) for 8, 16, 24 and 48 h. Then cells were harvested and stained with HO/PI, applied on glass slides, allowed to settle to the surface and then cells were counted under a microscope using a DAPI filter and cell death was determined. “e apopt”: early apoptotic cells; “l apopt”: late apoptotic cells; “necro”: necrotic cells. Statistical analysis by *t*-test confirmed that the differences between apoptosis- and necrosis-rates after treatment with BR (\pm adenosine) for 48 h were significant ($P < 0.05$). (b) Cells were treated with saline (Co), adenosine (A), 5 μ M and 20 μ M BR (\pm adenosine) for 16 h, which was a time point at which cellular membranes were still intact to avoid leaking. Then cells were harvested and the intracellular ATP content was measured as described in ‘Methods’. Statistical analysis by *t*-test confirmed that the differences between ATP-levels after treatment with BR (\pm adenosine) were significant ($P < 0.05$). (c) Micrographs of HL-60 cells stained with Hoechst 33258 (HO) and propidium iodide (PI) after treatment with saline, 5 μ M BR, 20 μ M BR, and 20 μ M BR+800 μ M adenosine (panel A) for 48 h (1st, 2nd, 3rd and 4th slides, from left to right, respectively). Panel B shows HL-60 cells which were exposed to 55°C heat shock for increasing times. The nuclei of viable cells stain blue (the cytoplasm remains invisible). In an early phase of apoptosis condensed chromatin is visible as small round bodies which usually stain more intense blue with HO. Late apoptotic cells exhibit similar chromatin condensation but the colour shifts to pink due to PI intrusion through leaky membranes as a consequence of apoptosis progression. Upon 20 μ M BR treatment, or in response to heat shock, increasing numbers of cells show a pink colour but lack apoptotic (condensed) chromatin (necrotic cells). Panel C: HL-60 cells were exposed to heat shock treatment (55°C) for 1, 3 and 5 h and PARP expression and degradation was monitored by Western blotting. There is no apoptosis specific cleavage of PARP into the 89 kD product detectable. (d) Processing of Caspase 3 into the activated p20 poly-peptide. HL-60 cells were treated with saline (control) or increasing doses of BR \pm 800 μ M adenosine. 5 μ M and 10 μ M BR, which induce mainly apoptosis, trigger processing of caspase 3. 20 μ M and 40 μ M BR mainly provokes necrosis and this is also reflected by the reduced levels of activated caspase 3. In presence of adenosine also 20 μ M and 40 μ M BR activate caspase 3 and induce apoptosis. Equal sample loading was controlled by Ponceau S staining

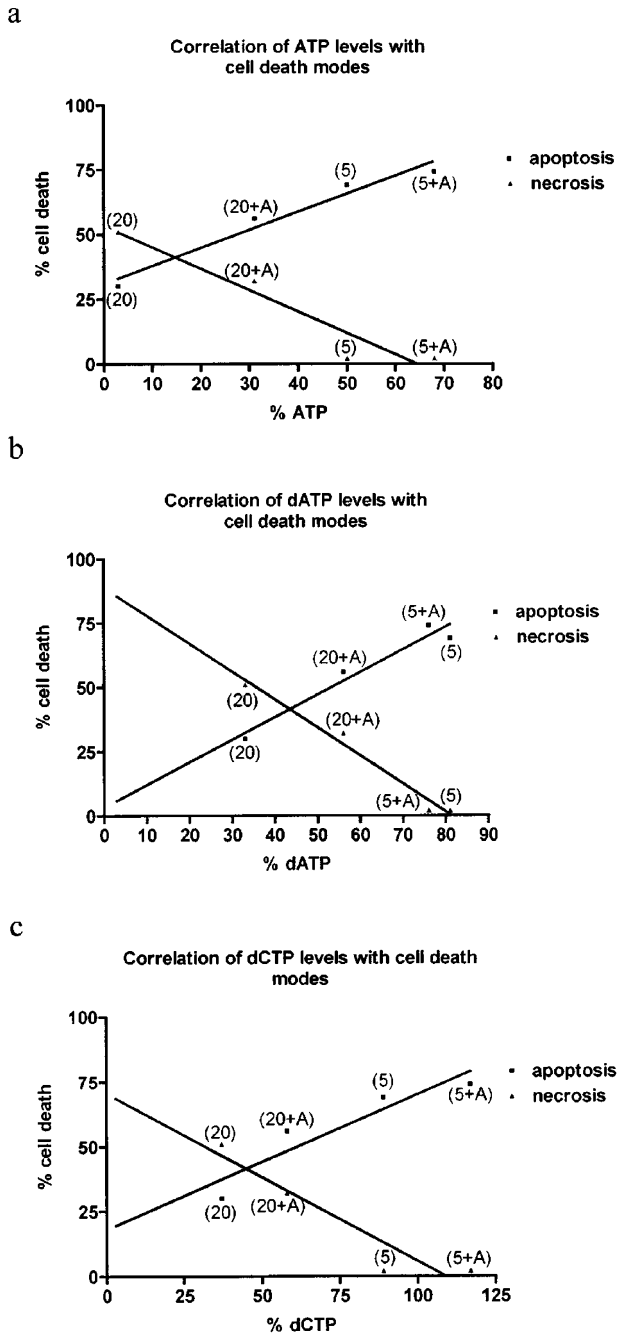


Figure 4 Correlation of nucleoside levels with cell death modes. HL-60 cells were treated with 5 μ M BR (5), 20 μ M BR (20), \pm adenosine (+A), for 16 h, which was a time point when membranes were still intact and at which cell death modes are already determined, to measure ATP- (a), dATP- (b), and dCTP-levels (c), and for 48 h to analyze cell death modes. These graphs demonstrate, that ATP, dATP, and dCTP levels correlate directly with the percentages of apoptotic cells, whereas ATP, dATP and dCTP levels correlate indirectly with the percentages of necrotic cells

levels might result in less dGTP-mediated feedback stimulation of ADP reduction by ribonucleotide reductase (RR). This in consequence decreases dADP levels and subsequently reduces dATP levels, which in fact was observed during treatment with BR. In turn, reduced dATP-

Treatment of HL-60 cells with cytotoxic drugs in combination with energy donors

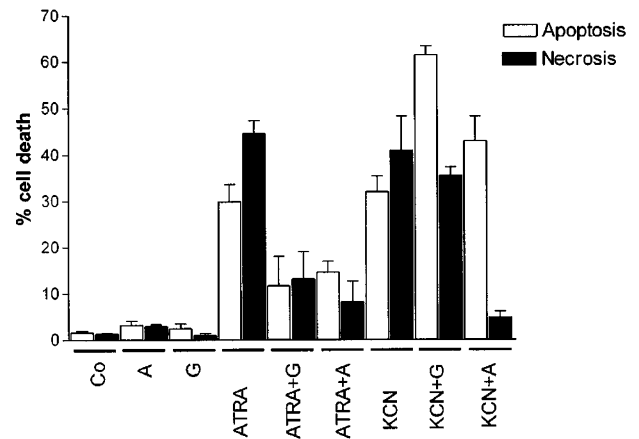


Figure 5 Modulations of cell deaths by adenosine and glucose. HL-60 cells were treated with saline (Co), 100 mM glucose (G), 800 μ M adenosine (A), 120 μ M all-trans retinoic acid (ATRA), 20 mM potassium cyanide (KCN) and combinations of ATRA or KCN with glucose and adenosine for 48 h. Then the type of cell death was determined by HOPI double-staining. Statistical analysis by *t*-test confirmed that the differences between apoptosis- and necrosis-rates versus respective controls were significant ($P < 0.05$)

mediated feedback inhibition of UDP-reduction by RR causes high dUDP and dUMP levels and this might be the reason for the observed increase in dTTP levels following BR treatment, because dUMP is the substrate for thymidylate synthase. Whereas there was no dose response correlation between ATP- and dATP-levels to total cell death, there was a direct correlation of these nucleotide pools to apoptosis and an indirect correlation to necrosis. Thus, ATP and/or dATP levels seem to determine cell death modes as it was previously suggested by others.^{15,24,25,39,42}

In earlier investigations it was demonstrated that BR suppressed survival pathways, induced apoptosis-relevant genes^{13,14} and activated Caspase 8 but not Caspase 9 (Polgar *et al.*, submitted). However, only low doses of BR (5 and 10 μ M), but not high doses (20 μ M and more) induced apoptosis by a pathway that culminated in Caspase 3 activation. At high BR-concentrations the majority of cell death was by necrosis presumably due to massive DNA damage. DNA double-strand breaks became rapidly repaired but a substantial amount of single-strand breaks and/or alkali-labile sites remained non-repaired. Surprisingly adenosine enabled a substantial number of the 20 μ M BR-treated cells, which contained massive DNA damage (23%), to escape necrosis and to undergo an apoptotic pathway (Table 2; Figure 6b). This percentage would correspond to cells with a DNA tail length between $>25 \mu$ m and $<87 \mu$ m.

DNA repair processes consume energy, particularly PARP, which is an enzyme involved in DNA repair and that becomes activated in response to DNA strand breaks.^{43,44} PARP consumes NAD as a substrate⁴⁵ and finally the cell depletes its ATP in an attempt to replenish its NAD pool.^{23,33,34,44,46} Thus, it is likely, that the necrotic

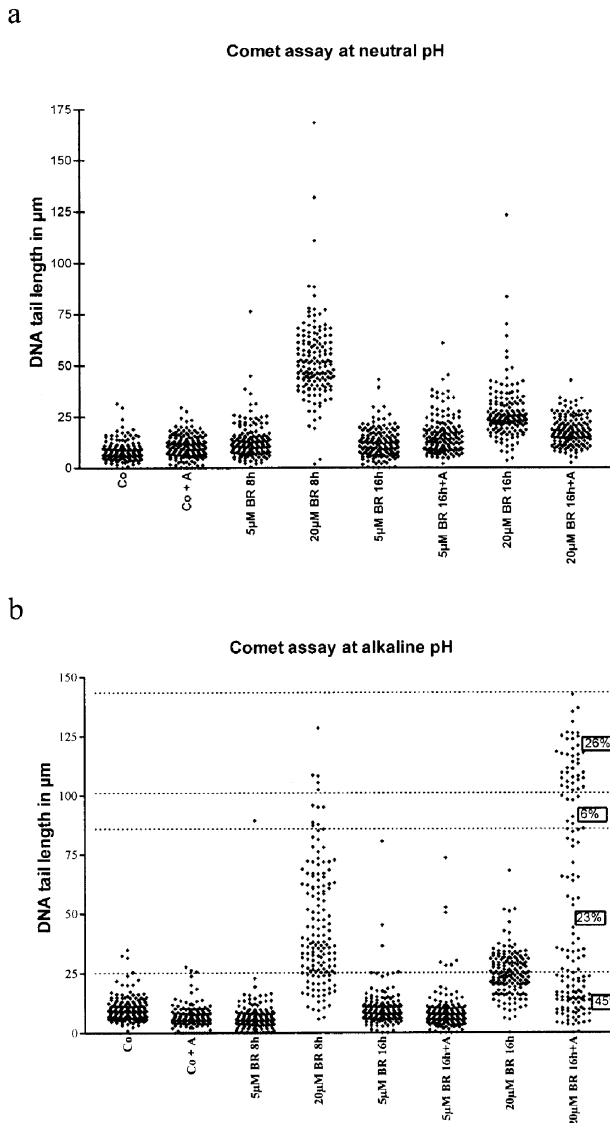


Figure 6 Induction of DNA damage in HL-60 cells by benzamide riboside (BR). Cells were treated with saline (Co), adenosine (Co+A), 5 µM, and 20 µM BR, ± adenosine, for 8 and 16 h. Then cells were harvested for comet analysis at neutral (a) and alkaline (b) pH and the extent of DNA migration was measured as described in Materials and Methods. Per experimental point three cultures were made in parallel and from each culture 50 cells were evaluated. The figures show the distribution pattern of 150 cells. The values in rectangles (b) give the per cent of cells between the dotted lines, which were treated with 20 µM BR+adenosine. The observed differences in DNA tail length between Co and 20 µM BR treatment for 8 and 16 h ± adenosine, are significant under neutral and alkaline conditions

damage arising from high BR concentrations are a consequence of DNA strand breaks and subsequent loss of ATP, which would have been required for an orchestrated apoptotic programme. Since maintenance of ATP by adenosine or supplementation with glucose, which is the major energy source of a cell, could prevent necrosis and favoured apoptosis, therefore, ATP and possibly also dATP are determinants of cell death modes.

This investigation supports the assumption, that energy donors can promote apoptosis and repress necrosis when

Cell death modulation by 3-AB

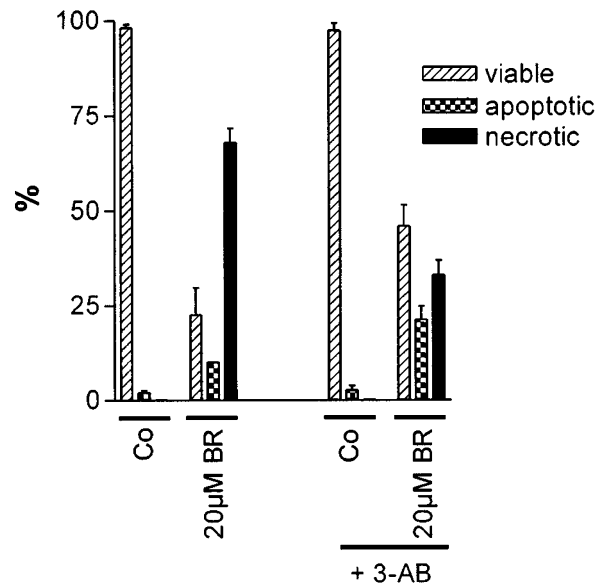


Figure 7 Prevention of necrosis by 3-AB. HL-60 cells were treated with saline (Co) and 20 µM BR, ± 3-amino benzamide (3-AB) for 48 h. Then the cell status was analyzed by HOPI double-staining. The reduced necrosis rates after treatment with 20 µM BR+3-AB are significant ($P < 0.05$), whereas the increased apoptosis rates are not ($P = 0.084$)

cell death is induced by various cytotoxic and therapeutic agents.

Materials and Methods

Chemicals

BR was synthesized as described earlier.¹ Polyclonal Caspase 3 antibody was purchased from Research Diagnostics (Flanders, NJ, USA), adenosine, glucose, 3-amino benzamide (3-AB), all trans retinoic acid (ATRA) and cyanide (KCN) were from Sigma (St. Louis, MO, USA).

Cell culture

The HL-60 human acute promyelocytic leukaemia cell line was from ATCC (Rockville, MD, USA). Cells were grown in RPMI 1640 medium (Gibco, Grand Island, NY, USA) with 10% heat inactivated FCS (Boehringer Mannheim GmbH, Mannheim, Germany) and 2 mM L-Glutamine (Gibco, Gaithersburg, MD, USA) in humidified atmosphere with 5% CO₂ at 37°C.

Hoechst 33258 propidium iodide (HOPI) double-staining

Hoechst 33258 (HO; Sigma) and propidium iodide (PI; Sigma) were added directly to the culture medium to final concentrations of 5 µg/ml and 2 µg/ml, respectively. After an incubation period of 1 h at 37°C, the cells were examined under a Zeiss Axiovert 35 fluorescence microscope with DAPI filters. Cells were photographed on Kodak

Ektachrome P1600 film (Eastman Kodak Company, Rochester, NY, USA) and viable, apoptotic, and necrotic cells were counted manually. The Hoechst dye stains the nuclei of all cells and therefore allows to monitor nuclear changes associated with apoptosis, such as chromatin condensation and nuclear fragmentation (Figure 3c). PI, on the other hand, is excluded from viable and early apoptotic cells, consequently PI uptake indicates loss of membrane integrity characteristic of necrotic and late apoptotic cells. In combination with fluorescence microscopy, the selective uptake of the two dyes allows the monitoring of the induction of apoptosis in intact cultures and to distinguish it from non-apoptotic cell death (necrosis). Necrosis is characterised in this system by nuclear PI uptake without chromatin condensation or nuclear fragmentation.

Electron microscopy

For transmission electron microscopy (TEM) cells treated with PBS (controls), 5 or 20 μ M BR for 24 h were fixed with 2.5% glutaraldehyde (in 0.1 M sodium cacodylate buffer with 4% sucrose, pH 7.2) for 45 min, washed in sodium cacodylate buffer and post-fixed in 2% osmium tetroxide (in 0.1 M sodium cacodylate buffer with 4% sucrose) for 45 min. Following several washes, the cells were concentrated by centrifugation at 150 *g* for 5 min, dehydrated in a graded series of ethanol, washed in propylene oxide, embedded in Epon (Serva, Germany) and sectioned at about 70 nm. The ultra-thin sections were stained with uranyl acetate/lead citrate for observation with a Zeiss EM 902 transmission electron microscope.

ATP assay

ATP content was measured with the ATP bioluminescence assay kit HS II from Boehringer Mannheim (Roche Molecular Biochemicals, Mannheim, Germany). Cells were treated with adenosine and BR for 16 h, subsequently their viability was measured by Trypan blue exclusion. There were <10% dead cells in each sample. 2.5 million cells were pelleted for each measurement and resuspended in 50 μ l dilution buffer. Equal amount of cell lysis reagent was then added and after an incubation period of 5 min at room temperature the samples were transferred to microtiter plates. Luciferase reagent (100 μ l) was added and the signal was detected immediately on a Lumi Imager F1 (Roche). Experiments were done in triplicates and the values of treated samples calculated as per cent of untreated controls.

Western blots

Cells from treated and untreated cultures were sedimented, washed in cold PBS, and lysed in SDS sample buffer (25 mM TRIS pH 6.8, 3% SDS, 10% glycerol, 36 mM DTT, 0.925 mM EDTA). Equal amounts of protein (calculated with the Dot Metric Protein Assay Kit from Novus Molecular, San Diego, CA, USA) were loaded onto 10 or 15% polyacrylamide gels. Proteins were electrophoresed at 80 V for 2–3 h and then transblotted onto PVDF membranes (Hybond P, Amersham International, UK) at 80 V for 2 h.⁴⁷ Membranes were quenched in PBS with 0.5% skim milk and 0.05% Tween 20 for 1 h, incubated with primary antibodies (mouse monoclonal anti PARP C-2-10 used 1:2000, mouse monoclonal anti gelosin used 1:2000, Sigma; rabbit polyclonal anti caspase 3 antibody used 1:1000, Research Diagnostics) overnight at 4°C and with horse radish peroxidase conjugated secondary antibody for 2 h at room temperature. The ECL Kit (Amersham International, UK) was used for blot development, chemiluminescence was detected on Kodak Xomat UV films.

Deoxyribonucleotide extraction and measurement

dNTPs were extracted as described previously⁴⁸ with trichloroacetic acid (TCA) 10% final concentration) followed by neutralization by triethylamine and 1,1,2-trichlorotrifluoroethane (1:4) mixture. The TCA extract was dried using a Speedvac drying system at room temperature and, if necessary, stored at –20°C until analysis. The assay for dNTP, which is based on the original DNA-polymerase assay,⁴⁹ was optimized by the use of 96-well plates⁵⁰ and tailor-made oligonucleotides,^{51,52} and was performed as previously described for dCTP.⁴⁸ After reconstitution of the samples in HEPES-buffered assay buffer (pH 7.3) at 10⁷ cells/ml, samples and standards (0, 1, 2.5 and 5 pmol dNTP) were added to diethylaminoethyl (DEAE) filter plates (Millipore, Ettenleur, The Netherlands). This was followed by addition of demi water (up to 30 μ l) and 70 μ l of a reaction mix, consisting of 10 μ l [8-³H]dATP (25 μ M; 1.6 Ci/mmol; 0.04 μ Ci/ μ l) for detection of dCTP, dTTP and dGTP and 10 μ l [CH₃-³H]dTTP (25 μ M, 1.6 Ci/mmol, 0.04 μ Ci/ μ l) for dATP detection, 5 μ l appropriate oligonucleotide (6 μ M, consisting of a primer attached to one of four possible templates specially designed for the detection of one of the four dNTPs), 5 μ l Klenow DNA pol I and 50 μ l assay buffer. The filterplates were gently vortexed and incubated at room temperature for 2 h. The wells were washed, the wet filters punched out and radioactivity counted as described.⁴⁸

Comet assay and statistical analysis

Neutral and alkaline single cell gel electrophoresis (SCGE) assays were carried out following the protocol described by Singh *et al.*⁵³ To measure DNA double-strand breaks electrophoresis was carried out under neutral conditions at pH 7.5,⁵⁴ to analyze single-strand breaks the electrophoresis was carried out under alkaline conditions at pH 13.0.⁵⁵ HL-60 cells were treated with BR and adenosine for 16 h, then the viability of the cells was determined with Trypan blue. All cultures which were used for Comet analysis had a viability of >90%. Pellets obtained upon centrifugation were mixed with 100 μ l low melting agarose (0.5%, 37°C) and spread on agarose coated slides according to Klaude *et al.*⁵⁶ Subsequently, the slides were exposed to lysis buffer⁵³ and transferred to neutral and alkaline electrophoresis buffer respectively for 40 min to allow unwinding of DNA. Thereafter, electrophoresis was carried out for 40 min (300 mA, 25 V) at pH 7.5 and 13.0 respectively. Finally the slides were stained with ethidium bromide and evaluated under a fluorescence microscope (Nikon Model: 027012) with an automated image analysis system.⁵⁷ For each experimental point, three cultures were evaluated and from each culture the tail lengths of 50 cells were determined. Statistically significant ($P < 0.05$) differences were determined with one way ANOVA.⁵⁷

Acknowledgements

We wish to thank Anton Jäger for his excellent technical assistance in preparing the figures. Grant support: This work was supported in part by the Herzfelder'sche Familienstiftung, the AICR-grant No. 97-12, the Anton Dreher Memorial Foundation to G Krupitza and by Austrian National Bank Fonds No. 8260 and the Hochschuljubiläumsfonds to T Szekeres.

References

1. Krohn K, Heins H and Wielckens K (1992) Synthesis and cytotoxic activity of C-glycosidic nicotinamide riboside analogues. *J. Med. Chem.* 35: 511–517

2. Jayaram HN, Gharehbaghi K, Jayaram NR, Rieser J, Krohn K and Paull KD (1992) Cytotoxicity of a new IMP dehydrogenase inhibitor, benzamide riboside, to human myelogenous leukemia K562 cells. *Biochem Biophys Res Commun* 186: 1600–1606
3. Gharehbaghi K, Sreenath A, Hao Z, Paull KD, Szekeres T, Cooney DA, Krohn K and Jayaram HN (1994) Comparison of biochemical parameters of benzamide riboside, a new inhibitor of IMP dehydrogenase, with tiazofurin and selenazofurin. *Biochem. Pharmacol.* 48: 1413–1419
4. Jackson RC, Weber G and Morris HP (1997) IMP dehydrogenase, an enzyme linked with proliferation and malignancy. *Nature* 256: 331–333
5. Weber G (1983) Biochemical strategy of cancer cells and the design of chemotherapy: G.H.A. Clowes Memorial Lecture. *Cancer Res.* 43: 3466–3492
6. Jayaram HN, Zhen W and Gharehbaghi K (1993) Biochemical consequences of resistance to tiazofurin in human myelogenous leukemic K562 cells. *Cancer Res.* 53: 2344–2348
7. Knight RD, Mangum J, Lucas DL, Cooney DA, Khan EC and Wright DG (1987) Inosine monophosphate dehydrogenase and myeloid cell maturation. *Blood* 69: 634–639
8. Jayaram HN, Dion RL, Glazer RI, Johns DG, Robins RK, Srivastava PC and Cooney DA (1982) Initial studies on the mechanism of action of a new oncolytic thiazole nucleoside, 2-beta-D-ribofuranosylthiazole-4-carboxamide (NSC 286193). *Biochem. Pharmacol.* 31: 2371–2380
9. Tricot GJ, Jayaram HN, Lapis E, Natsumeda Y, Nichols CR, Kneebone P, Heerema N, Weber G and Hoffman R (1989) Biochemically directed therapy of leukemia with tiazofurin, a selective blocker of inosine 5'-phosphate dehydrogenase activity. *Cancer Res.* 49: 3696–3701
10. Wright DG, Boosalis MS, Waraska K, Oshry LJ, Weintraub LR and Vosburgh E (1996) Tiazofurin effects on IMP-dehydrogenase activity and expression in the leukemia cells of patients with CML blast crisis. *Anticancer Res.* 16: 3349–3351
11. Jayaram HN, Lapis E, Tricot G, Kneebone P, Paulik E, Zhen W, Engeler GP, Hoffman R and Weber G (1992) Clinical pharmacokinetic study of tiazofurin administered as a 1-hour infusion. *Int. J. Cancer* 51: 182–188
12. Gharehbaghi K, Paull KD, Kelley JA, Barchi Jr JJ, Marquez VE, Cooney DA, Monks A, Scudiero D, Krohn K and Jayaram HN (1994) Cytotoxicity and characterization of an active metabolite of benzamide riboside, a novel inhibitor of IMP dehydrogenase. *Int. J. Cancer* 56: 892–899
13. Jayaram HN, Cooney DA and Grusch M (1999) Consequences of IMP dehydrogenase inhibition, and its relationship to cancer and apoptosis. *Curr. Med. Chem.* 6: 561–574
14. Grusch M, Rosenberger G, Fuhrmann G, Braun K, Titscher B, Szekeres T, Fritzer-Szekeres M, Oberhuber G, Krohn K, Hengstschlaeger M, Krupitza G and Jayaram HN (1999) Benzamide riboside induces apoptosis independent of Cdc25A expression in human ovarian carcinoma N.1 cells. *Cell Death Differ.* 6: 736–744
15. Tsujimoto Y (1997) Apoptosis and necrosis: Intracellular ATP level as a determinant for cell death modes. *Cell Death Differ.* 4: 429–434
16. Nicotera P, Leist M and Ferrando-May E (1998) Intracellular ATP, a switch in the decision between apoptosis and necrosis. *Toxicol. Lett.* 102: 139–142
17. Formigli L, Papucci L, Tani A, Schiavone N, Tempestini A, Orlandini GE, Capaccioli S and Orlandini SZ (2000) Aponecrosis: morphological and biochemical exploration of a synthetic process of cell death sharing apoptosis and necrosis. *J. Cell. Physiol.* 182: 41–49
18. Leist M and Nicotera P (1997) The shape of cell death. *Biochem. Biophys. Res. Commun.* 236: 1–9
19. Samali A, Nordgren H, Zhivotovsky B, Peterson E and Orrenius S (1999) A comparative study of apoptosis and necrosis in HepG2 cells: oxidant-induced caspase inactivation leads to necrosis. *Biochem. Biophys. Res. Commun.* 255: 6–11
20. Rosenberger G, Fuhrmann G, Grusch M, Fassi S, Elford HL, Smid K, Peters GJ, Szekeres T and Krupitza G (2000) The ribonucleotide reductase inhibitor trimidox induces c-myc and apoptosis of human ovarian carcinoma cells. *Life Sci.* 67: 3131–3142
21. Kothakota S, Azuma T, Reinhard C, Klippel A, Tang J, Chu K, McGarry TJ, Kirschner MW, Kohts K, Kwiatkowski DJ and Williams LT (1997) Caspase-3-generated fragment of gelsolin: effector of morphological change in apoptosis. *Science* 278: 294–298
22. Grusch M, Fritzer-Szekeres M, Fuhrmann G, Rosenberger G, Luxbacher C, Elford HL, Smid K, Peters GJ, Szekeres T and Krupitza G (2001) Activation of caspases and induction of apoptosis by amidox and didox. *Exp. Hematol.* in press
23. Ha HC and Snyder SH (1999) Poly(ADP-ribose) polymerase is a mediator of necrotic cell death by ATP depletion. *Proc. Natl. Acad. Sci. USA* 96: 13978–13982
24. Nicotera P and Leist M (1997) Energy supply and the shape of death in neurons and lymphoid cells. *Cell Death Differ.* 4: 435–442
25. Leist M, Single B, Castoldi AF, Kuhnle S and Nicotera P (1997) Intracellular adenosine triphosphate (ATP) concentration: a switch in the decision between apoptosis and necrosis. *J. Exp. Med.* 185: 1481–1486
26. Leist M, Single B, Naumann H, Fava E, Simon B, Kuhnle S and Nicotera P (1999) Inhibition of mitochondrial ATP generation by nitric oxide switches apoptosis to necrosis. *Exp. Cell. Res.* 249: 396–403
27. Petronini PG, Urbani S, Alfieri R, Borghetti AF and Guidotti GG (1996) Cell susceptibility to apoptosis by glutamine deprivation and rescue: survival and apoptotic death in cultured lymphoma-leukemia cell lines. *J. Cell. Physiol.* 169: 175–185
28. Fritzer-Szekeres M, Grusch M, Luxbacher C, Horvath S, Krupitza G, Elford HL and Szekeres T (2000) Trimidox, an inhibitor of ribonucleotide reductase, induces apoptosis and activates caspases in HL-60 promyelocytic leukemia cells. *Exp. Hematol.* 28: 924–930
29. Castaigne S, Chomienne C, Daniel MT, Ballerini P, Berger R, Fenau P and Degos L (1990) All-trans retinoic acid as a differentiation therapy for acute promyelocytic leukemia. I. Clinical results. *Blood* 76: 1704–1709
30. Fernandez PA, Rotello RJ, Rangini Z, Doupe A, Drexler HC and Yuan J (1994) Expression of a specific marker of avian programmed cell death in both apoptosis and necrosis. *Proc. Natl. Acad. Sci. USA* 91: 8641–8645
31. Nicotera P, Thor H and Orrenius S (1989) Cytosolic-free Ca²⁺ and cell killing in hepatoma 1c1c7 cells exposed to chemical anoxia. *FASEB J.* 3: 59–64
32. Shimizu S, Eguchi Y, Kamiike W, Waguri S, Uchiyama Y, Matsuda H and Tsujimoto Y (1996) Bcl-2 blocks loss of mitochondrial membrane potential while ICE inhibitors act at a different step during inhibition of death induced by respiratory chain inhibitors. *Oncogene* 13: 21–29
33. Lee YJ and Shacter E (1999) Oxidative stress inhibits apoptosis in human lymphoma cells. *J. Biol. Chem.* 274: 19792–19798
34. Filipovic DM, Meng X and Reeves WB (1999) Inhibition of PARP prevents oxidant-induced necrosis but not apoptosis in LLC-PK1 cells. *Am. J. Physiol.* 277: F428–436
35. Kim JW, Won J, Sohn S and Joe CO (2000) DNA-binding activity of the N-terminal cleavage product of poly(ADP-ribose) polymerase is required for UV mediated apoptosis. *J. Cell. Sci.* 113: 955–961
36. Watson AJ, Askew JN and Benson RS (1995) Poly(adenosine diphosphate ribose) polymerase inhibition prevents necrosis induced by H₂O₂ but not apoptosis. *Gastroenterology* 109: 472–482
37. Eliasson MJ, Sampei K, Mandir AS, Hurn PD, Traystman RJ, Bao J, Pieper A, Wang ZQ, Dawson TM, Snyder SH and Dawson VL (1997) Poly(ADP-ribose) polymerase gene disruption renders mice resistant to cerebral ischemia. *Nat. Med.* 3: 1089–1095
38. Finstad HS, Kolset SO, Holme JA, Wiger R, Farrants AK, Blomhoff R and Drevon CA (1994) Effect of n-3 and n-6 fatty acids on proliferation and differentiation of promyelocytic leukemic HL-60 cells. *Blood* 84: 3799–3809
39. Eguchi Y, Shimizu S and Tsujimoto Y (1997) Intracellular ATP levels determine cell death fate by apoptosis or necrosis. *Cancer Res.* 57: 1835–1840
40. Hunakova L, Duraj J, Romanova D, Novotny L, Sedlak J, Kelley MR, Szekeres T, Jayaram HN and Chorvath B (1998) Staurosporine enhanced benzamide riboside-induced apoptosis in human multidrug-resistant promyelocytic leukemia cells (HL-60/VCR) in vitro. *Neoplasma* 45: 204–209
41. Vitale M, Zamai L, Mazzotti G, Cataldi A and Falcieri E (1993) Differential kinetics of propidium iodide uptake in apoptotic and necrotic thymocytes. *Histochemistry* 100: 223–229
42. Lieberthal W, Menza SA and Levine JS (1998) Graded ATP depletion can cause necrosis or apoptosis of cultured mouse proximal tubular cells. *Am. J. Physiol.* 274: F315–327.
43. Juarez-Salinas H, Sims JL and Jacobson MK (1979) Poly(ADP-ribose) levels in carcinogen-treated cells. *Nature* 282: 740–741
44. Wielckens K, Schmidt A, George E, Bredehorst R and Hilz H (1982) DNA fragmentation and NAD depletion. Their relation to the turnover of endogenous mono(ADP-ribosyl) and poly(ADP-ribosyl) proteins. *J. Biol. Chem.* 257: 12872–12877
45. Ueda K and Hayaishi O (1985) ADP-ribosylation. *Annu. Rev. Biochem.* 54: 73–100

46. Althaus FR and Richter C (1987) ADP-ribosylation of proteins. Enzymology and biological significance. *Mol. Biol. Biochem. Biophys.* 37: 1–237
47. Towbin H, Staehelin T and Gordon J (1979) Electrophoretic transfer of proteins from polyacrylamide gels to nitrocellulose sheets: procedure and some applications. *Proc. Natl. Acad. Sci. USA* 76: 4350–4354
48. van Moorsel CJ, Pinedo HM, Veerman G, Guechev A, Smid K, Loves WJ, Vermorken JB, Postmus PE and Peters GJ (1999) Combination chemotherapy studies with gemcitabine and etoposide in non-small cell lung and ovarian cancer cell lines. *Biochem. Pharmacol.* 57: 407–415
49. Hunting D and Henderson JF (1981) Determination of deoxyribonucleoside triphosphates using DNA polymerase: a critical evaluation. *Can. J. Biochem.* 59: 723–727
50. Peters GJ, De Abreu RA, Oosterhof A and Veerkamp JH (1983) Concentration of nucleotides and deoxynucleotides in peripheral and phytohemagglutinin-stimulated mammalian lymphocytes. Effects of adenosine and deoxyadenosine. *Biochim. Biophys. Acta* 759: 7–15
51. Sherman PA and Fyfe JA (1989) Enzymatic assay for deoxyribonucleoside triphosphates using synthetic oligonucleotides as template primers. *Anal. Biochem.* 180: 222–226
52. Iwasaki H, Huang P, Keating MJ and Plunkett W (1997) Differential incorporation of ara-C, gemcitabine, and fludarabine into replicating and repairing DNA in proliferating human leukemia cells. *Blood* 90: 270–278
53. Singh NP, McCoy MT, Tice RR and Schneider EL (1988) A simple technique for quantitation of low levels of DNA damage in individual cells. *Exp. Cell Res.* 175: 184–191
54. Olive PL, Wlodek D and Banath JP (1991) DNA double-strand breaks measured in individual cells subjected to gel electrophoresis. *Cancer Res.* 51: 4671–4676
55. Tice RR and Strauss GH (1995) The single cell gel electrophoresis/comet assay: a potential tool for detecting radiation-induced DNA damage in humans. *Stem Cells* 13 Suppl 1: 207–214
56. Klaude M, Eriksson S, Nygren J and Ahnstrom G (1996) The comet assay: mechanisms and technical considerations. *Mutat. Res.* 363: 89–96
57. Uhl M, Helma C and Knasmuller S (2000) Evaluation of the single cell gel electrophoresis assay with human hepatoma (Hep G2) cells. *Mutat. Res.* 468: 213–225